Supporting Information

Regulating catalytic kinetics in nanoclimbing-wall-like NiO/NiCoP hybrids for enhanced overall water splitting

Xiuwen Wang[a*], Lan Yu[a], Chunmei Lv[a], Ying Xie[b], Yanqing Jiao[b*], Wen Xin[a], Tengfei Xu[a], Tingting Su[a], and Libin Yang[a*]

[a] Heilongjiang Provincial Key Laboratory of Surface Active Agent and Auxiliary, Qiqihar University, Qiqihar, 161006, China.

Email: xwwang@qqhru.edu.cn, yanglibin@qqhru.edu.cn.

[b] Key Laboratory of Functional Inorganic Material Chemistry, Ministry of Education, Heilongjiang University, Harbin, 150080, China.

Email: jiaoyanqing@hlju.edu.cn.

Experimental details

Materials

All chemicals involved in experiments were of analytical grade and used without further purification. The cobalt nitrate hexahydrate ($Co(NO_3)_2·6H_2O$), nickel nitrate hexahydrate ($Ni(NO_3)_2·6H_2O$), natrium acetate (CH_3COONa), potassium hydroxide (KOH), and sodium hypophosphite (NaH_2PO_2) were obtained from Shanghai Aladdin Bio-chemical Technology Co. Ltd. The hydrochloric acid (1M HCl), anhydrous ethanol (AR), and acetone were obtained from Tianjin Kemiou Chemical Reagent Co., Ltd. Nickel foam (NF) was purchased from Suzhou Taili Material Technology Co. Ltd. The ultrapure water (>18 MΩ cm^{-1}) was used throughout the experiments.

Synthesis of NiCo-LDH/NF

A piece of nickel foam (NF, 3×3 cm) was precleaned by acetone, 1 M HCl, and deionized water. In a typical synthesis, 4 mmol $Co(NO_3)_2·6H_2O$, 4 mmol $Ni(NO_3)_2·6H_2O$, and 12 mmol CH_3COONa were dissolved in 30 mL of ultrapure water, respectively. Then, the above mixed solution and NF was transferred to Teflon-lined autoclave (50 mL) and maintained at 150 ℃ for 10 h. After it cooled down to the room temperature, the NF was covered with blue-green solids, suggesting the formation of NiCoOH precursor on NF (named as NiCo-LDH/NF). The resulting NiCo-LDH/NF was washed with ethanol and ultrapure water several times, and then dried in an oven at 60 ℃.

Synthesis of NiO/NiCoP/NF

The as-prepared NiCo-LDH/NF and NaH_2PO_2 (0.5 g) were placed on the downstream and upstream of the porcelain tube, respectively. The furnace was heated at 350 ℃ for 2 h with a heating speed of 2 ℃/min in nitrogen atmosphere. After natural cooling, the obtained sample (marked as NiCoP/NF) was ultrasonically cleaned for 30 s and washed with ultrapure water for several times to remove the surface adsorbed NaH_2PO_2. Subsequently, the NiCoP/NF was annealed at 400 ℃ for 4 h with a heating rate of 2 ℃/min in air atmosphere, then the target product (NiO/NiCoP/NF) can be obtained. The mass loading of NiO/NiCoP/NF was ~ 3.6 mg/cm^2.

Synthesis of comparative electrocatalysts

The preparation of NiCoP/NiO/NF was similar to that of NiO/NiCoP/NF, except that the NiCo-LDH/NF undergoes the continuous oxidation and phosphorization treatments.

The synthesis of NiCoP/NF and NiO/NF were similar to that of NiO/NiCoP/NF, except that the NiCo-LDH/NF undergoes the phosphorization and oxidation, respectively.

The preparation of NiCoP-0.2/NF and NiCoP-1.0/NF was similar to that of NiCoP/NF, except that the mass of NaH_2PO_2 was changed to 0.2 g and 1.0 g, respectively.

The synthesis of NiO/NF-350 and NiO/NF-450 was similar to that of NiO/NF, except that the reaction temperature changed to the 350 ℃ and 450 ℃, respectively.

Characterization

X-ray diffraction (XRD) patterns were recorded on an X-ray diffractometer (Rigaku D/max-IIIB, Cu Kα, λ=1.5406 Å) at a scan rate of 10° min^{-1} in the range from 10° to 80°. The chemical composition measurements were performed by X-ray photoelectron spectroscopy (XPS, X-ray source energy: 1486.7eV, binding energy calibration: 284.6 eV, background pressure: 4×10^{-9} Pa) using Al Kα radiation. Scanning electron microscopy (SEM) were carried out by using a Hitachi S-4800 microscope. Transmission electron microscopy (TEM), high-resolution TEM (HRTEM), and element mapping were obtained from JEM-3010 (JEOL, Japan) with a voltage of 200 kV.

Electrochemical tests

Electrochemical tests were conducted on a CHI760E electrochemical workstation (Shanghai Chenhua Instrument Corp., Shanghai, China). The as-prepared NiCoP/NiO/NF, NiO/NiCoP/NF, NiCoP/NF, and NiO/NF can be used directly as working electrode. The graphite rod and the standard Hg/HgO electrode were used as counter electrode and reference electrode, respectively. Linear sweep voltammogram (LSV) was conducted at a 5 mV s^{-1} scan rate after 20 cycles of CV tests to stabilize the current. A 90 % *iR* compensation was employed in the electrochemical measurement of LSV. CV was carried out with scan rates of 0, 20, 30, 40, 50 mV s^{-1} to assess the electrochemical double-layer capacitance (C_{dl}) within non-Faradaic potential range. The electrochemical impedance spectroscopy (EIS) data can be obtained at the frequency range of 0.01-100,000 Hz. Long-term stability was evaluated by performing 1000 cycles of CV at a scan rate of 100 mV s^{-1} over selected potential ranges. The chronoamperometry current density-time (I-t) curves were conducted under controlled

potentials for 48 h. The volumes of hydrogen and oxygen produced during the electrocatalytic reaction were collected using the drainage method. In the solar driven water splitting part, the entire system consists of a commercial solar cell (size: 8×8 cm) and electrolyzer under the light intensity of 100 mW/cm^2 (AM 1.5 G). The equation of $STH\%=(J\times1.23\ V)/100\ mW\ cm^{-2}$ was used to calculate the efficiency of STH.

Computational details

All calculations based on density functional theory (DFT) were carried out using the Vienna ab initio simulation package (VASP)[1]. Perdew-Burke-Ernzerhof functional with a generalized gradient approximation (GGA-PBE) form was adopted to deal with the exchange correlation energies of the systems[2]. The plane-wave and pseudo-potential techniques were used, and the energy cutoff was 400 eV. To obtain a good numerical sampling of electron densities in Brillouin zone, a (6×6×8) Monkhorst-Pack mesh was applied to the NiCoP and a (8×8×8) to NiO. The (2×2×1) Monkhorst-Pack mesh was applied to the NiCoP (201), NiO (202), and NiCoP (201)/NiO (202) surface. The optimization procedure was repeated until the maximum residual force is less than 0.05 eV·Å^{-1} in any directions. During the calculations, a vacuum layer of 15 Å is used to avoid the fake interactions between periodic images along z axis. Visualization of the atomic structures are made by using VESTA[3]. The NiCoP (201), NiO (202), and NiCoP (201)/NiO (202) were simulated to investigate the mechanism of HER and OER under alkaline electrolyte conditions. The adsorption Gibbs free energy of reaction intermediates (ΔG) is defined as:

$$\Delta G = \Delta E + \Delta E_{ZPE} - T\Delta S$$

where ΔE is the DFT energy difference of each step, ΔE_{ZPE} is the correction of zero point energy, ΔS is the variation of entropy obtained by vibration analysis, T is the temperature (T = 298.15 K).

References:

1. G. Kresse and J. Furthmüller, *Phys. Rev. B*, 1996, **54**, 11169-11186.

2. B. Hammer, L. B. Hansen and J. K. Nørskov, *Phys. Rev. B*, 1999, **59**, 7413-7421.

3. K. Momma and F. Izumi, *J. Appl. Crystall.*, 2011, **44**, 1272-1276.

Supporting data

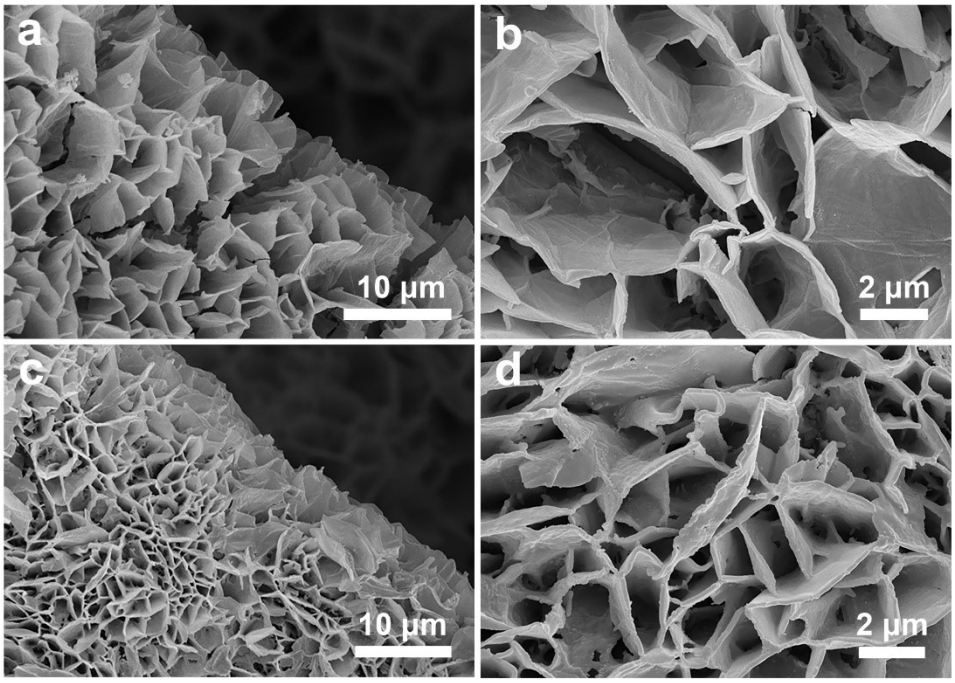

Fig. S1 SEM images of NiCoP/NF-0.2 (a, b) and NiCoP/NF-1.0 (c, d).

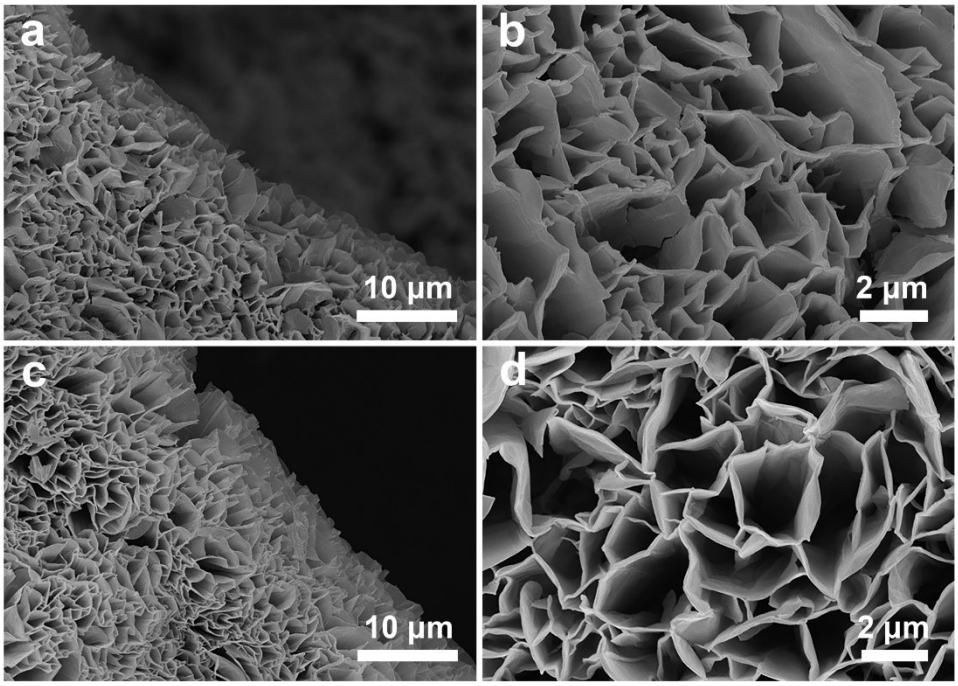

Fig. S2 SEM images of NiO/NF-350 (a, b) and NiO/NF-450 (c, d).

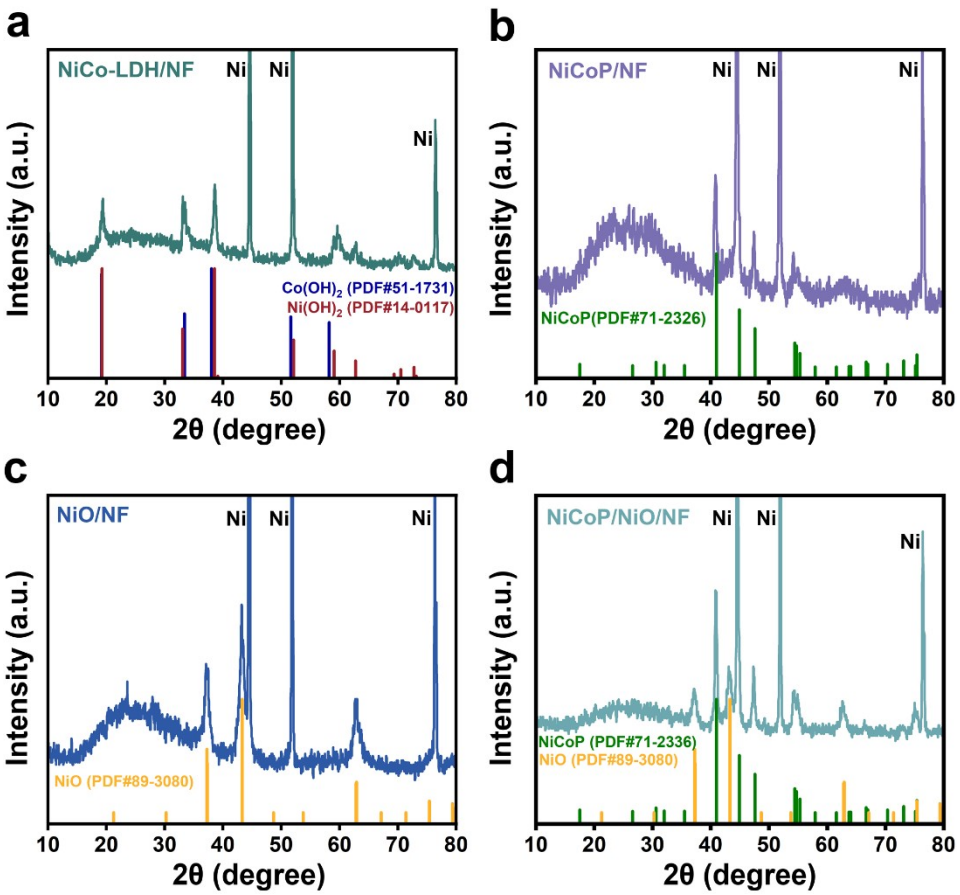

Fig. S3 XRD patterns of obtained NiCo-LDH/NF (a), NiCoP/NF (b), NiO/NF (c), and NiCoP/NiO/NF (d), respectively.

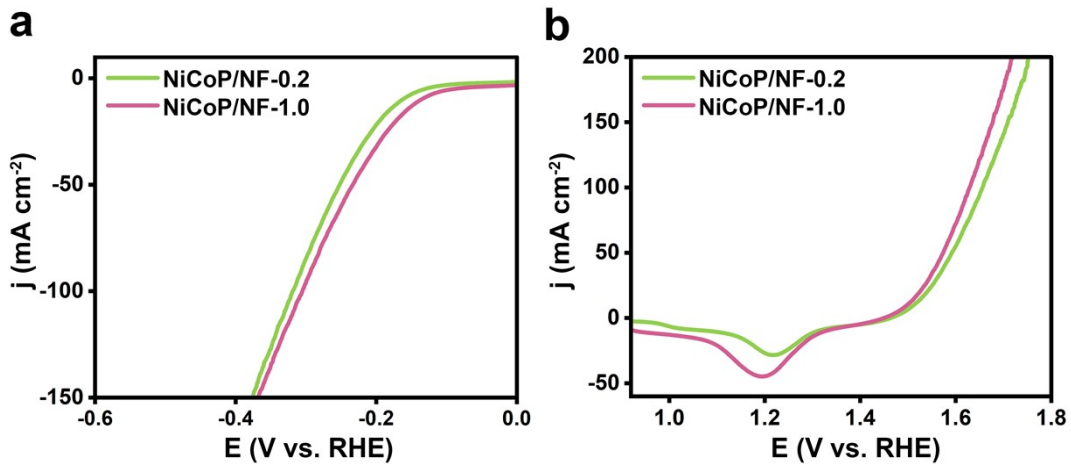

Fig. S4 LSV curves of NiCoP/NF-0.2 and NiCoP/NF-1.0 for alkaline HER (a) and OER (b).

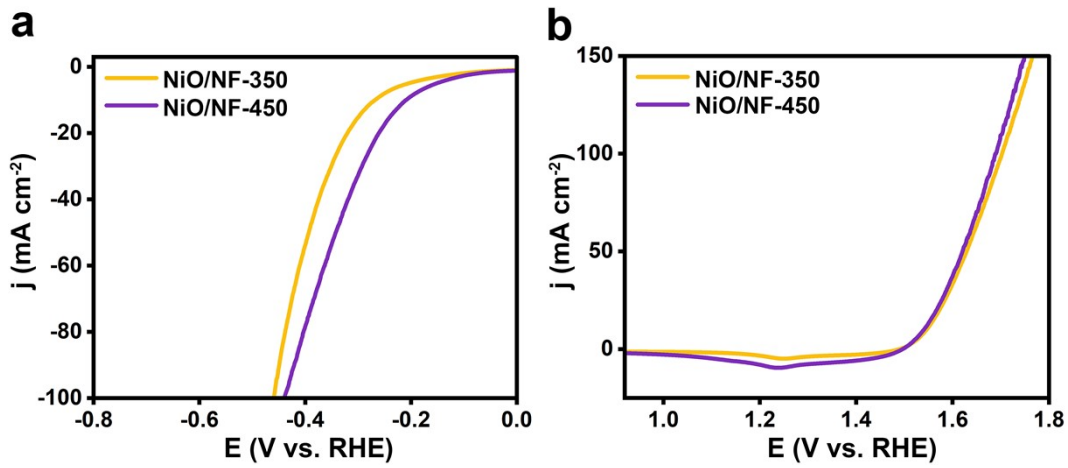

Fig. S5 LSV curves of NiCo-LDH/NF with different oxidation temperature for alkaline HER (a) and OER (b).

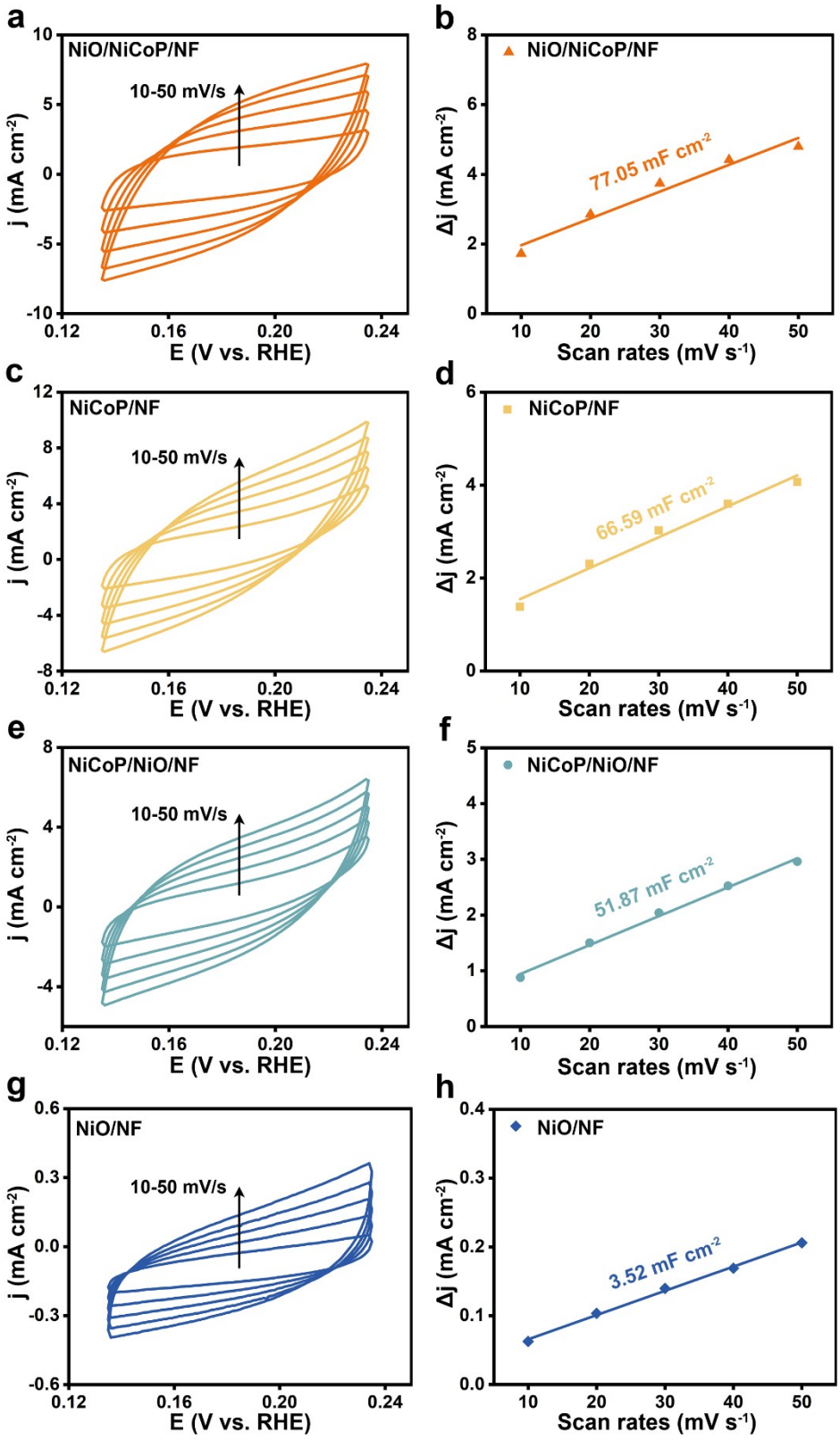

Fig. S6 CV curves of as-prepared catalysts with scan rates ranging from 10 mV/s to 50 mV/s and the corresponding C_{dl} for alkaline HER.

Table S1 Electrochemical performance parameters of various electrocatalysts for HER.

CEs	η_{10}(mV)	Tafel (mV dec^{-1})	R_{ct} (Ω)	τ_e (s)	C_{dl} (mF cm^{-2})
NiO/NiCoP/NF	92	92.84	1.85	60.98×10^{-3}	77.05
NiCoP/NF	119	133.62	2.22	34.29×10^{-3}	66.59
NiCoP/NiO/NF	133	138.75	6.24	8.95×10-3	51.87
NiO/NF	149	197.58	7.53	8.85×10^{-3}	3.52
Pt/C	38	-	-	-	-

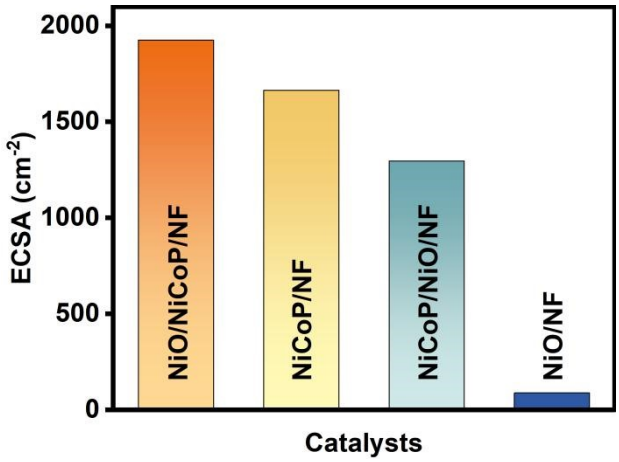

Fig. S7 ECSA values of NiO/NiCoP/NF, NiCoP/NF, NiCoP/NiO/NF, and NiO/NF for alkaline HER.

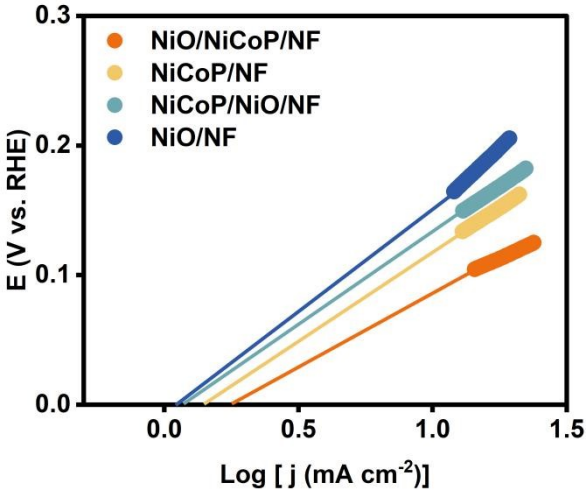

Fig. S8 Exchange current density of NiO/NiCoP/NF, NiCoP/NF, NiCoP/NiO/NF, and NiO/NF in 1 M KOH for HER.

Table S2 Comparison of HER activity with cobalt- or nickel-based electrocatalysts, which was consisted with the listed references in **Fig. 3f**.

Catalysts	η_{10}(mV)	References
Co_2P/Ni_2P/NF	51	Mater. Today Phys. 2021, 16, 100314.
Ni_2P/NPC-P	73	ACS Appl. Mater. Interfaces 2022, 14, 18, 20358-20367.
CoNi/NF-P	113.3	Mol. Catal. 2023, 547, 113327.
Co-Ni-P	119	Electrochim. Acta 2021, 381, 138286.
NiCo-NiCoP@PCT	135	Chem. Eng. J. 2021, 426, 129214.
CoP@FeCoP/NC YSMPs	141	Chem. Eng. J. 2021, 403, 126312.
CoP@CoP@$(Co/Ni)_2$	147	Chem. Eng. J. 2023, 463, 142448.
CoP@NCNFs	166	J. Colloid Interface Sci. 2022, 616, 379-388.
Ni1Co1-P	169	J. Alloy. Compd. 2020, 847, 156514.
15%W-$Ni_{12}P_5$	172	ACS Appl. Mater. Interfaces 2022, 14, 581-589.
CoP@NC/NCNT	177	J. Colloid Interface Sci. 2023, 629, 22-32.
$Co(OH)_2$	182	Energy Fuels 2022, 36, 7006-7016.
$Co(OH)_2/Fe_7Se_8$	183	Chem. Eng. J. 2023, 466, 143124.
Fe_2P/Co@NPC	235	J. Mater. Chem. A. 2022, 10, 16037-16045.
NiO/NiCoP/NF	**92**	**This work**

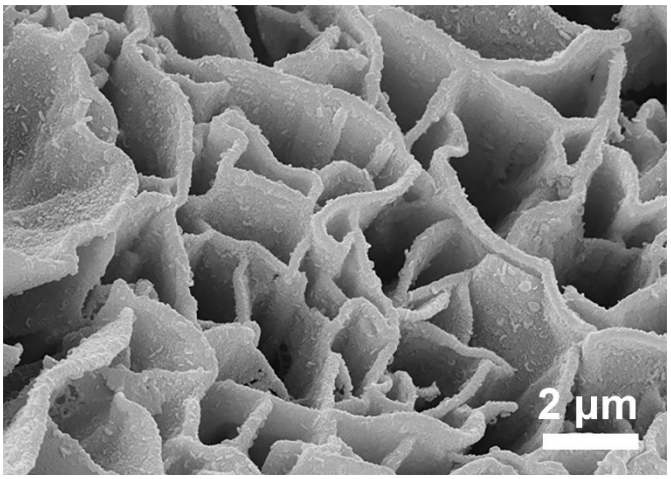

Fig. S9 SEM images of NiO/NiCoP/NF after HER stability test.

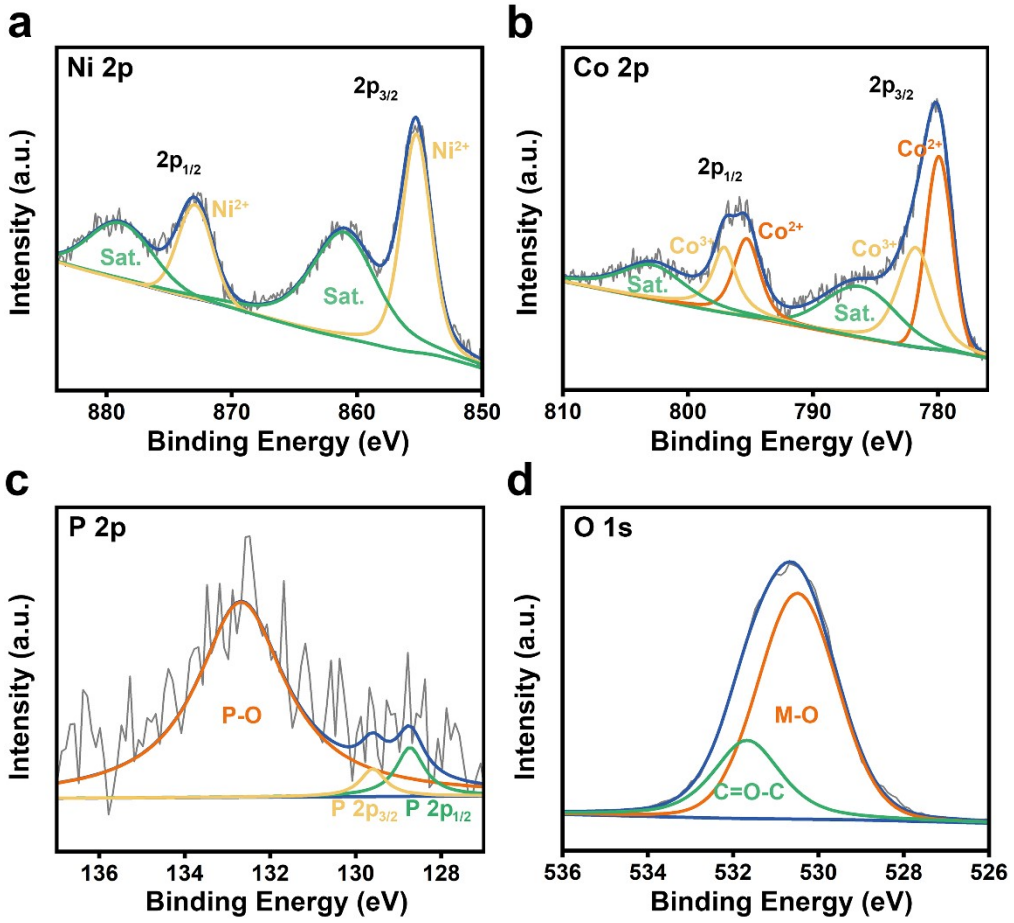

Fig. S10 High-resolution XPS spectra of Ni 2p (a), Co 2p (b), P 2p (c), and O 1s (d) of NiO/NiCoP/NF after HER stability.

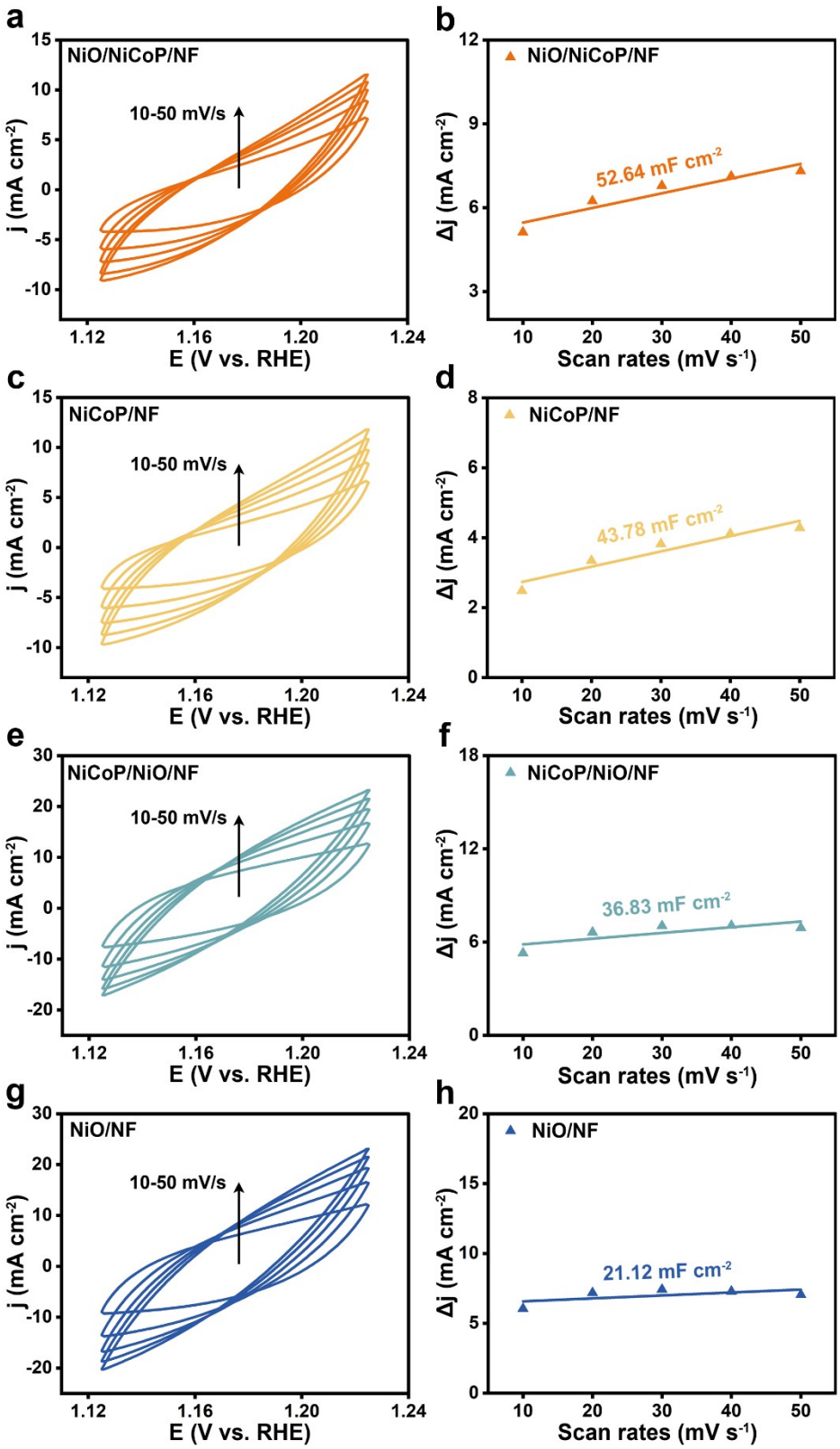

Fig. S11 CV curves of as-prepared catalysts with scan rates ranging from 10 mV/s to 50 mV/s and the corresponding C_{dl} for alkaline OER.

Table S3 Electrochemical performance parameters of various electrocatalysts for OER.

CEs	η_{10}(mV)	Tafel (mV dec^{-1})	R_{ct} (Ω)	τ_e (s)	C_{dl} (mF cm^{-2})
NiO/NiCoP/NF	216	72.33	0.83	5.03	52.64
NiCoP/NF	244	91.82	2.34	3.43	43.78
NiCoP/NiO/NF	263	122.35	3.69	2.83	36.83
NiO/NF	306	130.67	6.62	1.93	21.12
RuO_2	294	-	-	-	-

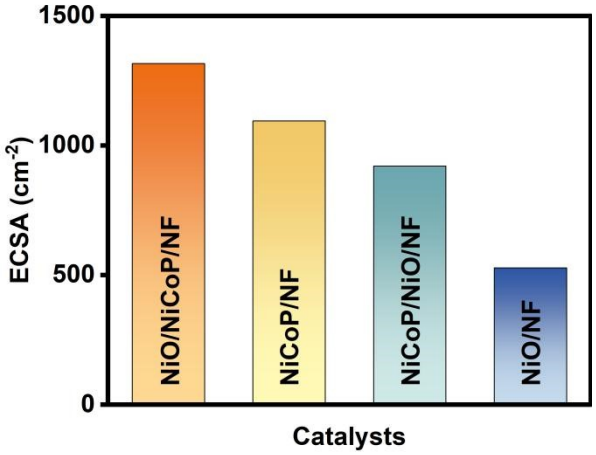

Fig. S12 ECSA values of NiO/NiCoP/NF, NiCoP/NF, NiCoP/NiO/NF, and NiO/NF for alkaline OER.

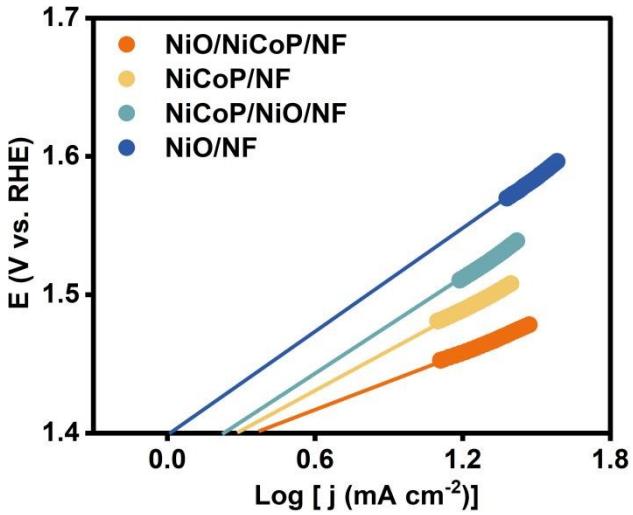

Fig. S13 Exchange current density of NiO/NiCoP/NF, NiCoP/NF, NiCoP/NiO/NF, and NiO/NF in 1 M KOH for OER.

Table S4 Comparison of alkaline OER activity with cobalt- or nickel-based electrocatalysts, which was consisted with the listed references in **Fig. 4f**.

Catalysts	η_{10}(mV)	References
NiFeP@N-CS	216	Appl. Surf. Sci. 2021, 549, 149297.
$Ni_{0.25}Co_{0.75}P$	240	Mater. Today Commun. 2024, 38, 108163.
$CoNi_2S_4/Ni_3S_2$/NF	243	J. Alloys Compd. 2020, 844, 156252.
MoP/NiFeP	256	Mater. Chem. Front. 2021, 5, 375.
NiFeP@C	260	ACS Appl. Mater. Interfaces. 2020, 12, 19447-19456.
NiCoP-WO_3	270	J. Mater. Chem. A. 2021, 9, 10909-10920.
Co-O NSs-2 nm	278	ACS Nano. 2023, 17, 5861-5870.
$Co(OH)_2$	281	Energy Fuels 2022, 36, 7006-7016.
$CoNiP_x$@$FeCoP_x$/C@$CoNiP_x$	289	Small. 2023, 19, 2302906.
Ni-Co_3O_4	300	RSC Adv. 2020, 10, 12962-12969.
CoP@NC/NCNT	324	J. Colloid Interface Sci. 2023, 629, 22-32.
Fe_2P/Co@NPC	331	J. Mater. Chem. A. 2022, 10, 16037-16045.
CoP@NCNFs	336	J. Colloid Interface Sci. 2022, 616, 379-388.
NiO/$NiCo_2O_4$/NF	336	J. Colloid Interface Sci. 2023, 643, 214-222.
NiO/NiCoP/NF	**216**	**This work**

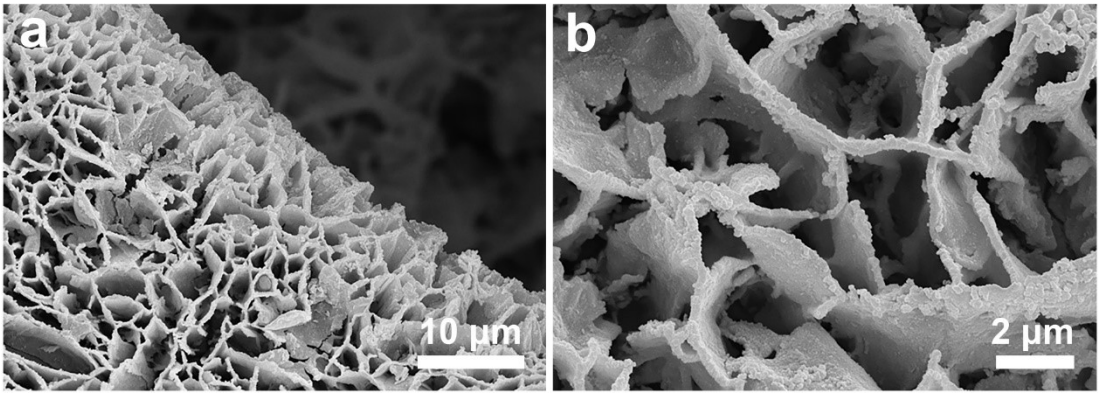

Fig. S14 SEM images of NiO/NiCoP/NF after OER stability test.

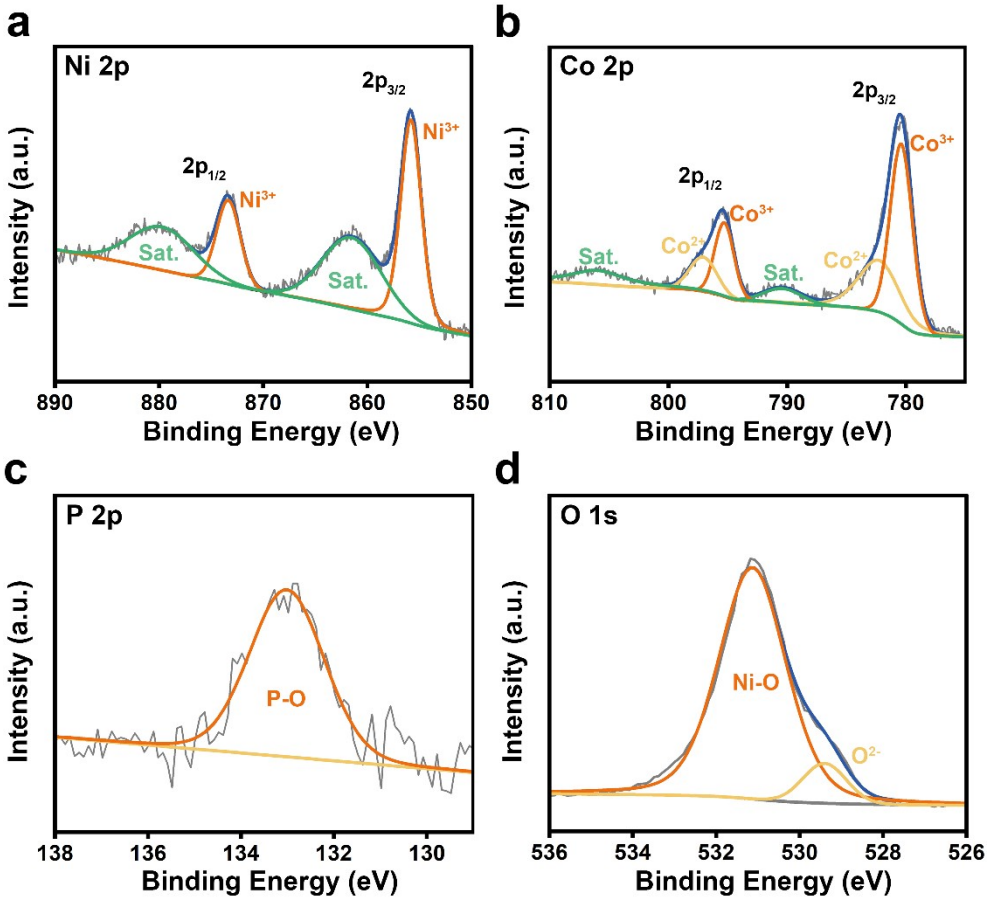

Fig. S15 High-resolution XPS spectra of Ni 2p (a), Co 2p (b), P 2p (c), O 1s (d) of NiO/NiCoP/NF after OER stability.

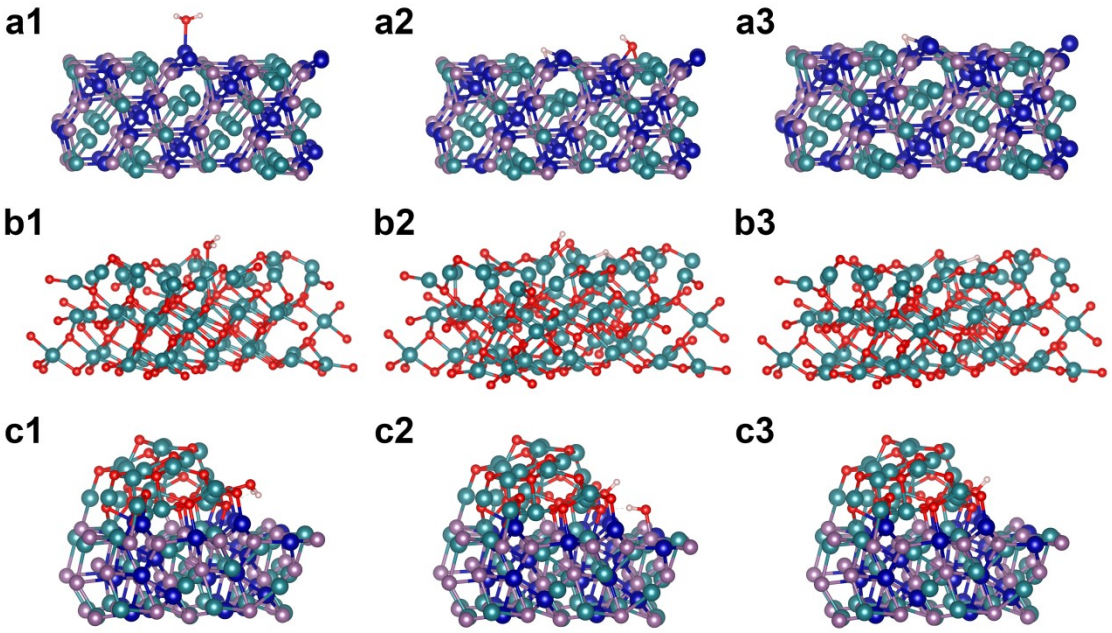

Fig. S16 The structure configuration of water, water dissociation intermediates, and H* adsorbed on NiCoP (a1-a3), NiO (b1-b3) and NiO/NiCoP (c1-c3), respectively. Notes: green, blue, pink, red, and white ball represent Ni, Co, P, O and H atom, respectively.

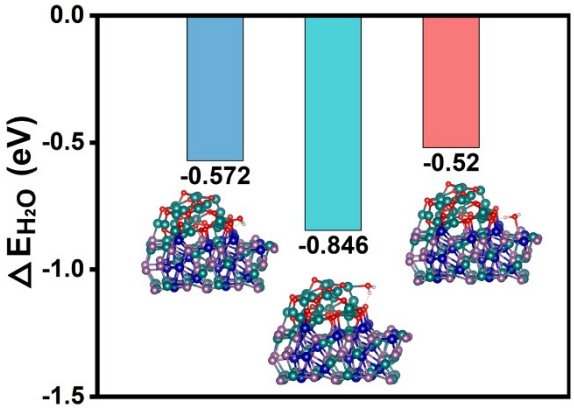

Fig. S17 The calculated ΔG_{H2O} values of different sites in NiO/NiCoP.

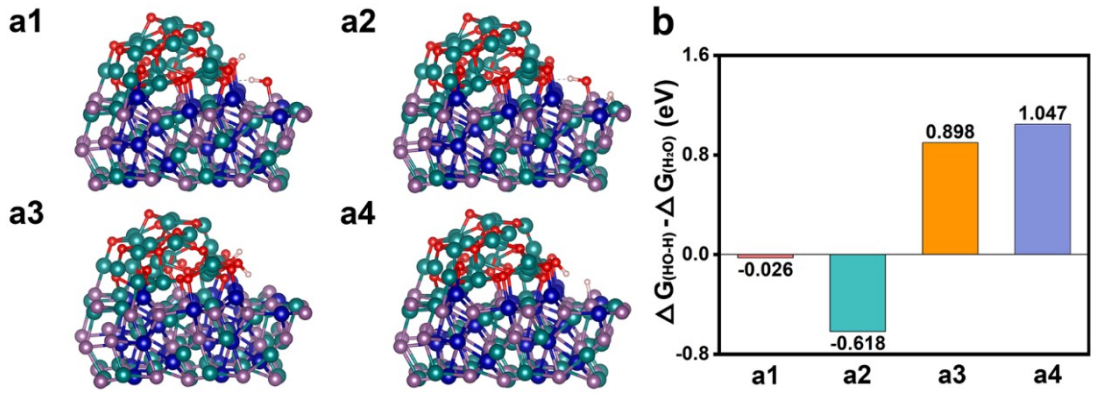

Fig. S18 The optimized structures of H_2O dissociation on different sites of NiO/NiCoP (a1-a4) and the corresponding energy barrier of H_2O dissociation (b).

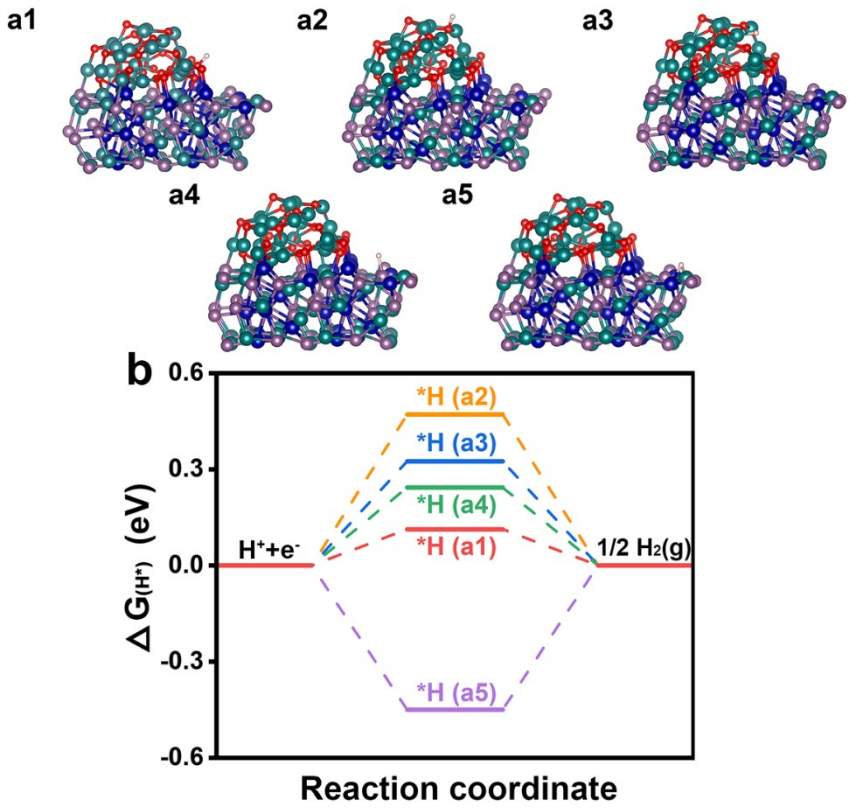

Fig. S19 The optimized structures of H* intermediates on different sites of NiO/NiCoP (a1-a5) and the corresponding free energy diagram (b).

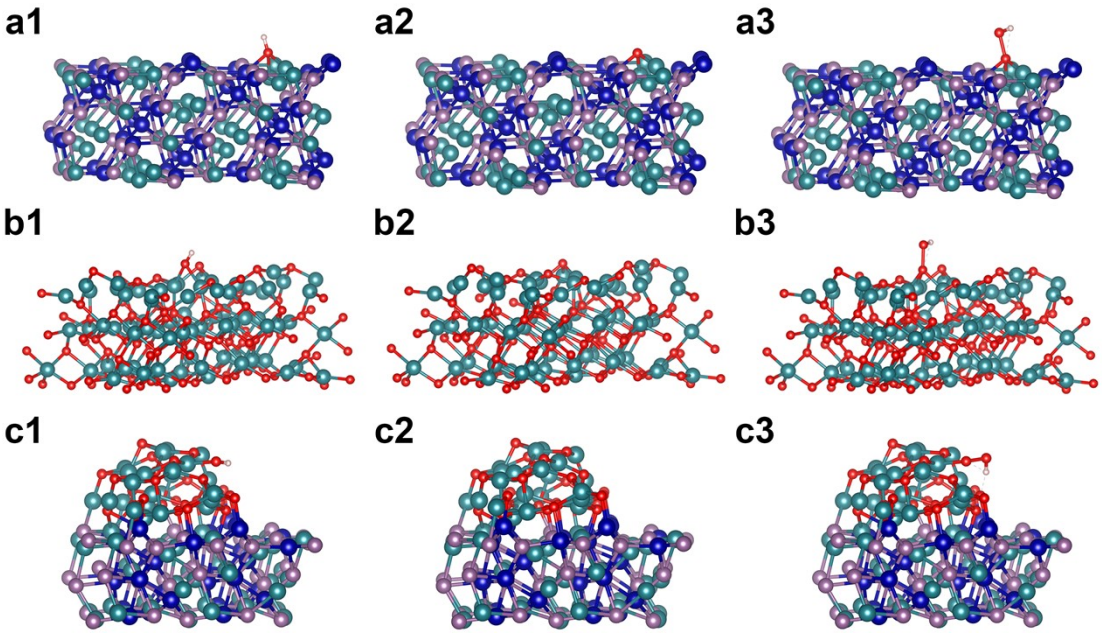

Fig. S20 The structure configuration of OH*, O*, and OOH* adsorbed on NiCoP (a1-a3), NiO (b1-b3) and NiO/NiCoP (c1-c3), respectively. Notes: green, blue, pink, red, and white ball represent Ni, Co, P, O and H atom, respectively.

Table S5 Comparison of overall water splitting performance of NiO/NiCoP/NF with recently non-noble metal bifunctional electrocatalysts in 1.0 M KOH.

Catalysts	Voltage (V)	References
CoP@CoOOH	1.52	Small 2022, 18, 2106012.
Ni_2P-Co_2P	1.54	Chem. Mater. 2021, 33, 9165.
O-NiMoP/NF	1.56	Adv. Funct. Mater. 2021, 31, 2104951.
MXene-NiCoP	1.57	ACS Appl. Mater. Interfaces 2020, 12, 18570-1577.
Co-Ni/Ni_3N	1.575	InfoMat. 2022, 4, e12251.
$CoNiFe_2O_4$@MXene	1.58	Fuel 2023, 346, 128305.
Ni/$Ni(OH)_2$	1.59	Adv. Mater. 2020, 32, 1906915.
$NiCo_2O_4$/Cu_xO/Cu	1.61	J. Mater. Chem. A 2021, 9, 14466-14476.
NiFeMo/NF	1.62	Appl. Surf. Sci. 2023, 607, 154803.
CoP/NFs	1.65	ACS Catal. 2020, 10, 412-419.
$Co(OH)_2$	1.65	Energy Fuels 2022, 36, 7006-7016.
CoP@NC/NCNT	1.72	J. Colloid Interface Sci. 2023, 629, 22-32.
Fe_2P/Co@NPC	1.73	J. Mater. Chem. A. 2022, 10, 16037-16045.
Co/N-CNFs	1.80	ACS Appl. Mater. Interfaces. 2022, 14, 4399-4408.
$Co_{0.25}Fe_{0.75}$-LDH	1.89	ACS Catal. 2023, 13, 1477-1491.
NiO/NiCoP/NF	**1.56**	**This work**